

NMR studies into colloidal stability and magnetic order in fatty acid stabilised aqueous magnetic fluids†

Swapankumar Ghosh,^{ab} Darren Carty,^a Sarah P. Clarke,^a Serena A. Corr,^c Renata Tekoriute,^c Yurii K. Gun'ko^c and Dermot F. Brougham^{*a}

Received 25th June 2010, Accepted 7th September 2010

DOI: 10.1039/c0cp00989j

We report the physico-chemical characterisation of fatty acid stabilised aqueous magnetic fluids, which are ideal systems for studying the influence of nanoparticle aggregation on the emergent magnetic resonance properties of the suspensions. Stable colloids of superparamagnetic magnetite, Fe₃O₄, nanoparticle clusters in the 80 to 100 nm size range were produced by *in situ* nanoparticle growth and stabilisation, and by suspending pre-formed nanoparticles. NMR relaxation analysis shows that the magnetic resonance properties of the two types of suspension differ substantially and provides new insights into how the relaxation mechanisms are determined by the organisation of the nanoparticles within the clusters.

Introduction

Aqueous suspensions of superparamagnetic nanoparticles have potential biomedical applications as platforms for drug delivery^{1,2} and as mediators for hyperthermia.³ This therapeutic potential is further enhanced by the possibility of localizing the magnetic particles in the body using externally applied magnetic fields, and/or detecting their presence by magnetic resonance imaging.⁴ Suspensions of this type have already found clinical application in diagnostic MRI,⁵ for instance in targeted imaging of cancer using off-resonance saturation methods.⁶ Furthermore, the suspensions offer the potential advantage of strong and tunable image contrast; for instance the increase in T_2 associated with particle aggregation could be exploited for diagnostic applications based on molecular recognition events.⁷

The extent of aggregation of magnetic fluids, and the nature of the aggregates, or clusters, is critical to their performance for most applications. In particular, aggregation has a strong influence on the magnetic resonance properties of the suspensions, as dipolar interactions between particles increase the effective magneto-crystalline anisotropy. Hence there is ongoing interest in studying the factors that determine aggregation. Berret and co-workers⁸ have recently reported the controlled preparation of clusters of superparamagnetic γ -Fe₂O₃ nanoparticles (NPs) with cationic–neutral copolymers and have assessed their potential as negative MRI contrast agents. Using *in situ* NP growth and stabilisation in the reaction of Fe salts with polysodium-4-styrene sulfonate, we have recently

shown⁹ that by varying the reactant ratio, superparamagnetic or partially magnetically blocked Fe₃O₄ nanocomposite suspensions can be prepared.

The aqueous alkanolic acid stabilised magnetic colloids are a group of model suspensions for which nanoparticle aggregation has been studied in detail. These suspensions are stabilised by a surface bilayer coating,¹⁰ composed of a primary chemisorbed layer with the carboxylate groups bound to the surface, and a secondary interpenetrating physisorbed layer with the hydrophilic head-groups pointing outwards. Extensive light and neutron scattering, and cryo-TEM studies¹¹ have shown that in aqueous suspension densely packed nanoparticle clusters are formed, which can be described as having a fractal dimension of ~ 2.5 . This detailed knowledge of the structures formed means that the suspensions are ideal systems for study using magnetic resonance techniques. NMR relaxation studies of fatty-acid stabilised suspension have recently been reported,¹² although that work was limited to the high frequency, clinical MRI, range.

The superparamagnetic relaxation enhancements due to the suspended particles are quantified by the relaxivity. The observed spin–lattice relaxation rate is given by;

$$R_{1,\text{obs}} = \frac{1}{T_{1,\text{obs}}} = R_{1,\text{dipolar}} + r_1[\text{Fe}] \quad (1)$$

where $R_{1,\text{dipolar}}$ is the observed water spin–lattice relaxation rate in the absence of a superparamagnetic enhancement, the iron concentration is given in mM. Thus the spin–lattice relaxivity, r_1 , a concentration independent measure of the efficacy of the agent, has units of $\text{s}^{-1} \text{mM}^{-1}$. The magnetic field dependence of the relaxivity can be measured in the range 0.25 mT to 0.5 T, which is equivalent to resonance frequency of 0.01 to 20 MHz for ¹H, using the technique of nuclear magnetic resonance dispersion, NMRD. The NMRD ‘profiles’ obtained are sensitive to the magnetic properties of the suspended material, and so provide more information than single-field measurements of r_1 . Hence the technique is increasingly being used to investigate magnetic nano-suspensions.^{9,13–15}

^a National Institute for Cellular Biotechnology, School of Chemical Sciences, Dublin City University, Dublin 9, Ireland.

E-mail: dermot.brougham@dcu.ie; Fax: +353 1 7005503; Tel: +353 1 7005472

^b Ceramics Division, National Institute for Interdisciplinary Science and Technology (NIIST), CSIR, Trivandrum, 695019, India

^c School of Chemistry and CRANN Institute, Trinity College, University of Dublin, Dublin 2, Ireland

† Electronic supplementary information (ESI) available: TEM, Raman spectra, XRD patterns and magnetisation curves. See DOI: 10.1039/c0cp00989j

The generally accepted theory for water relaxation due to superparamagnetic nanoparticles in suspension (SPM theory) was developed by Muller and co-workers.¹⁶ SPM theory extends classical outer-sphere theory of relaxation by including both a high Curie component, even at moderate fields, and strong magneto-crystalline anisotropy. The high frequency relaxation is driven by diffusion of water, with the position of the r_1 maximum determined by the characteristic correlation time for diffusive motion, τ_D . The low frequency relaxation is due to fluctuations in the particles moment, *i.e.* the Néel process. The effect of the saturation magnetisation, M_s , is largely to increase the relaxivity across the frequency range. Using physically acceptable values for the critical parameters (the particle size; saturation magnetisation, M_s ; the Néel correlation time, τ_N ; and the magnetocrystalline anisotropy energy, ΔE_{anis}), excellent agreement with the measured profiles of dispersed superparamagnetic nanoparticle suspensions can be obtained.^{14–16} A detailed description of the influence of the magnetic properties of the suspended nanoparticles on the NMRD profiles, and of SPM theory, has recently been presented.⁵

In this paper we report the preparation of aqueous alkanolic acid stabilised magnetic fluids both by suspending pre-formed solid Fe_3O_4 NPs, and by *in situ* Fe_3O_4 NP growth and stabilisation. The resulting clusters were found to be more stable to dilution than previously reported, due to improved control of the ligand coverage. The suspensions were characterised by dynamic light scattering (photon correlation spectroscopy) and, for the first time, NMRD. The effect of inter-particle interactions on the spin–spin relaxation is well documented,⁵ here we present the first detailed study into the effects of clustering on the spin–lattice relaxation. The insights gained into the stability of these model colloids, and the influence of inter-particle interactions on the magnetic resonance characteristics, are of interest given recent developments in smart MRI contrast agents which rely on particle aggregation.^{7,17} The understanding of the low-frequency ^1H NMR relaxation mechanisms that we develop may also be of interest to the growing field of micro-tesla MRI.¹⁸

Experimental

Materials

All reagents and Fe salts were obtained from Sigma-Aldrich and used without further purification. Fatty acids were obtained from Sigma-Aldrich (purity >99.9%), and again were used without further purification.

Synthetic procedures

Suspensions formed by *in situ* nanoparticle synthesis and coating (BPCs). Stable magnetic fluids were synthesised by a sequential process involving the *in situ* coating by the surfactant decanoic acid (C10:0) during chemical co-precipitation of Fe(II) and Fe(III) salts with ammonium hydroxide by following a minor modification of the method of Shen *et al.*,¹⁰ which itself is a modification of Wooding's method.¹⁹ A mixture of iron(III) chloride hexahydrate and iron(II) chloride tetrahydrate, in the molar ratio of 2 : 1 (typically 0.5 and 0.25 mmol),

were dissolved in 20 mL deoxygenated water. The solution was heated slowly to 80 °C with very strong magnetic stirring and maintained for 30 min at that temperature. One-fifth of the total of 0.4 mmol of primary surfactant was added (note that Shen *et al.* reported the addition of one-ninth of the total surfactant at this stage) to the solution at this time followed by immediate addition of the required volume 0.5 mL of 33% ammonia. The remaining surfactant (0.32 mmol) was then added to the mixture in five parts over 5 min; stirring was continued for another 15 min at 80 °C, the typical volume after all the additions was about 21 mL. The suspension was then cooled to room temperature and precipitated in one step by the sequential addition of equal volumes of acetone (25 mL) and methanol (25 mL). A black precipitate was separated by using a strong bar magnet to hold the solids and washing them alternately with acetone and methanol five times to remove all surfactants, except that part directly bonded to the particle surface. The washed particles disperse readily in non-polar organic solvents to produce concentrated non-aqueous dispersions. This synthetic procedure, and in particular this reaction temperature, has been shown to produce black superparamagnetic (*i.e.* sub 20 nm) magnetite, Fe_3O_4 , nanoparticles.^{10,11} The phase of the particles was confirmed by X-ray analysis and magnetometry, see ESI.†

To produce an aqueous suspension a secondary surfactant layer of the same or different surfactant is required.²⁰ The primary layer coated ultra fine nanoparticles were re-dispersed in water and the temperature of the suspension was raised to 60 °C with strong stirring. The second surfactant (0.25 mmol), usually lauric acid (C12:0) as its ammonium salt (pH \geq 10), was then added drop-wise to the suspension. The suspensions were then sonicated at 50 °C for several minutes. This procedure produced magnetite (Fe_3O_4) nanoparticles stabilised against agglomeration by bilayers of *n*-alkanoic acids with 9 to 13 carbons. The nanoparticle suspensions were characterised by PCS, NMRD and the primary NP size was determined by TEM. For the purposes of this article, suspensions prepared in this way will be referred to as fatty acid bilayer-coated nanoparticle clusters, or BPCs.

Suspensions formed by stabilisation of preformed uncoated nanoparticles (SPCs). Iron oxide nanoparticles were synthesised using previously published methods.²¹ Magnetometry and Raman spectroscopy were used to demonstrate that the particles are superparamagnetic magnetite, Fe_3O_4 , see ESI.† Magnetic fluids were prepared by suspending magnetite nanoparticles in water using sodium oleate or sodium decanoate (Sigma-Aldrich \sim 99%) as surfactants. For the suspensions reported here 4 mg of magnetite powder was added to 2 mg of sodium oleate, 5 mL water was then added to produce a suspension of *ca.* 5 mM Fe. The mixtures were then sonicated at 50 °C for 2 h. The stability of the fluids was confirmed by measuring their transmittance at 540 nm using a UV-Visible spectrometer over two months as well as by NMRD. The nanoparticle suspensions were characterised by PCS, NMRD and the primary NP size was determined by TEM. For the purposes of this article, suspensions prepared in this way will be referred to as fatty acid stabilised nanoparticle clusters, or SPCs.

Dynamic light scattering

The DLS measurements were performed on a HPPS particle sizer (Malvern Instruments, Malvern UK), using a detection angle of 173° at a temperature of 25°C . The HPPS uses a 3 mW He–Ne laser operating at a wavelength of 633 nm. The z -average, or mean hydrodynamic diameters (d_{hyd}) and the polydispersity index values (PDI is a measure of the distribution width) which are based upon the intensity of scattered light were calculated using cumulants analysis.²²

Electron microscopy

Transmission electron microscopy (TEM) images were taken on a Hitachi H-7000. The TEM was operated at a beam voltage of 100 kV. Samples for TEM were prepared by drying of a drop of suspension onto a formvar coated 400 mesh copper grid.

Nuclear magnetic resonance dispersion

The ^1H NMRD data were recorded using a Stellar Spinmaster, Fast Field Cycling Relaxometer (Stellar SRL, Mede, Italy).²³ The system was operated at a measurement frequency of 9.24 MHz for ^1H , with a 90° pulse of 7 μs . T_1 measurements were performed as a function of external field, B_0 , with standard pulse sequences incorporating B_0 field excursions.²⁴ A field switching rate of 20 MHz ms^{-1} ensured that measurement of T_1 relaxation times as low as 1 ms were possible, although the shortest T_1 value measured in this study was 3.1 ms. The field range covered was from 20 MHz to 1 kHz. Below 10 kHz local magnetic fields including the earth's field become significant. By application of a field compensation system,²⁵ we were able to compensate for the uncompensated local laboratory field. While this allows B_0 to be varied down to 0.1 kHz, we only present data from 1 kHz and above here. The ^1H magnetisation recovery curves were found to be mono-exponential, within the error, at all temperatures and frequencies, allowing determination of T_1 to a precision $\leq 1\%$

in all cases. The temperature of the samples was controlled with a precision of $\pm 1^\circ\text{C}$ with a thermostated airflow system.

Determination of iron content

Total iron content was determined by atomic absorption spectroscopy. Samples were prepared for analysis as follows. Concentrated HCl solution (0.5 mL) and 1 mL deionised H_2O was added to a small aliquot (typically 0.3–0.5 mL) of the nanoparticle suspension. The mixture was heated until only 1 drop of liquid remained, at which time 25 mL deionised water was added. The solution was heated to boiling, then immediately removed from heat and allowed to cool to room temperature. The volume was adjusted to 100 mL. Spectra were recorded on a Varian SpectrAA Spectrometer with a single slit burner. The light source was a Fe-cathode lamp with a wavelength of 248.3 nm. Control experiments, using the detergent Triton X-100 to ensure dissolution of the organic component,²⁶ confirmed that oleic acid and its conjugate base do not interfere with the iron determination. Typical iron concentrations obtained, for the samples analyzed by NMRD, were in the range of 2–12 mM.

Results

^1H NMR relaxation in BPC suspensions

Relaxivity data for a group of BPC water suspensions from different syntheses performed under identical conditions are shown in Fig. 1a. The NMRD results indicate good reproducibility for a synthesis involving many steps conducted over a period of two days. The deviation of r_1 (at 0.01 MHz) from the average is $\sim 12\%$. The d_{hyd} values of the suspensions were found to vary from 80–100 nm, which is far larger than the NP size. In all cases the cluster size distributions were uni-modal, with relatively low PDI values, ≤ 0.15 . For the suspension used to produce Fig. 1b, the d_{hyd} value was 82 nm, PDI 0.15.

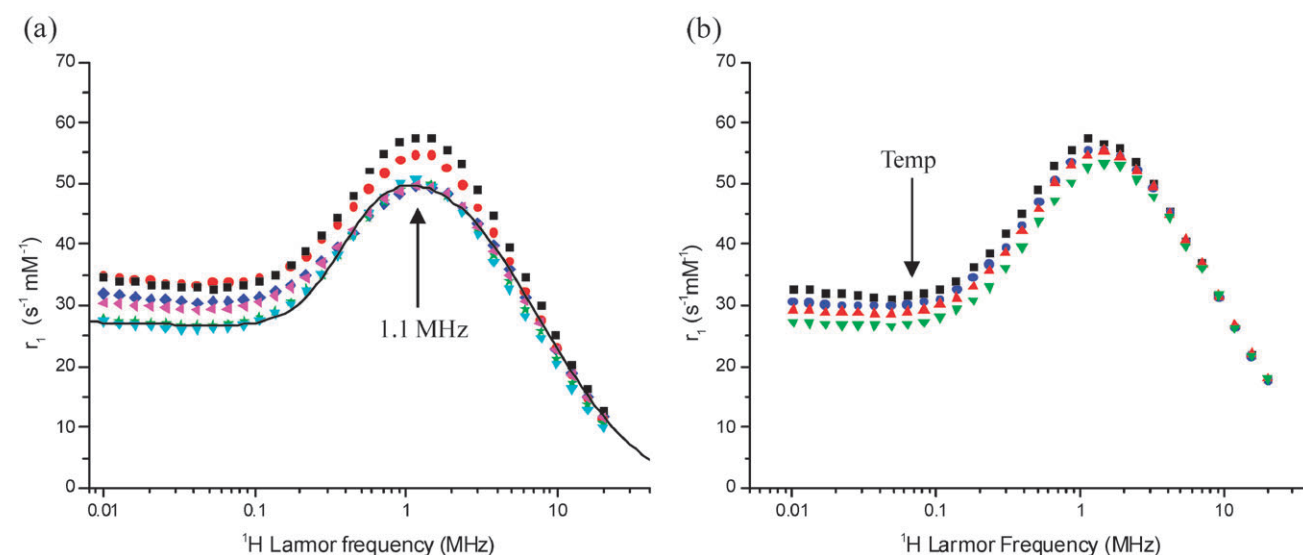


Fig. 1 (a) ^1H NMR relaxation profiles recorded in aqueous suspension at 25°C for six independently prepared BPC suspensions. In all cases the primary layer was (C10:0) and (C12:0) was used as the secondary surfactant. A simulated profile, using SPM theory, is shown as a solid line, the parameters used in the simulation were; $d_{\text{NMR}} = 20\text{ nm}$, $M_s = 27\text{ emu g}^{-1}$, $\Delta E_{\text{anis}} = 2.2\text{ GHz}$, $\tau_N = 24 \times 10^{-9}\text{ s}$. (b) Profiles recorded for a single typical BPC suspension, with average d_{hyd} 82 nm, PDI 0.15, at temperatures of 19°C ■, 23°C ●, 28°C ▲ and 33°C ▼.

Statistical analysis of TEM data for the sample demonstrates the presence of monodisperse nanoparticle of average size $d_{\text{NP}} = 10.6 \pm 1.6$ nm (ESI†).

The main features in the profiles; a low frequency r_1 plateau; a prominent maximum in the low MHz range; and a rapid decrease in r_1 at higher frequency, strongly suggest that the ^1H NMR relaxation is due to superparamagnetic nanoparticles in suspension. Simulations using SPM theory¹⁶ provide reasonable agreement with the experimental data, confirming the superparamagnetism. The frequency of the r_1 maximum (~ 1.1 MHz) suggests a primary particle size of about 20 nm. The saturation magnetisation, M_s , extracted is 27 emu g^{-1} . The ΔE_{anis} and τ_N values were in the low GHz and ns ranges, respectively, which is as expected. Increasing the temperature, from 19 to 33 °C, Fig. 1b, has little effect on the high frequency relaxivity, but results in a slight decrease in r_1 at low frequency. It should also be noted that the NMR and light scattering properties of the BPC suspensions were not changed by extended exposure, during the field-cycling experiment, to magnetic fields of 0.5 T.

^1H NMR relaxation in SPC suspensions

A SPC suspension with d_{hyd} 98 nm, PDI 0.19, formed from particles with $d_{\text{NP}} = 11.4 \pm 1.6$ nm, as indicated by TEM (see ESI†), was characterised by NMRD over a wide temperature range, selected data are presented in Fig. 2. The NMRD and light scattering properties were stable to thermal cycling at all temperatures up to 80 °C, and magnetic fields up to 0.5 T. In the temperature range up to about 50 °C, it is apparent that there are three frequency regimes, Fig. 2a. For Larmor frequencies below ~ 8 kHz (Regime I) the measured relaxivity decreases with temperature, but is almost independent of frequency. For Larmor frequencies from about 8 kHz to 3 MHz (Regime II) the relaxivity conforms to a power law dependence on frequency, where the power decreases with increasing temperature. Finally, for Larmor frequencies above

3 MHz (Regime III) the relaxivity is independent of temperature, in the range studied. In this regime the relaxivity is as expected for a dispersed suspension of superparamagnetic nanoparticles; the relaxation mechanism is essentially outer-sphere.^{4,16}

On increasing the temperature above 50 °C, Fig. 2b, the frequency and temperature dependencies of the relaxivity in Regimes I and III are similar to those observed for BPCs. The clearest change with temperature is in the intermediate frequency range, Regime II 8 kHz–3 MHz, where there is a deviation from the power law dependence of r_1 on frequency, indicative of a change in the relaxation mechanism. On raising the temperature to 70 °C, a weak maximum in r_1 , at 1–2 MHz, becomes apparent. This suggests the onset of superparamagnetic ^1H NMR relaxation.

Effect of pH on ^1H NMR relaxation in magnetic nanoparticle cluster suspensions

Further confirmation that the relaxation mechanism changes, for both BPC and SPC suspensions, at frequencies below 3 MHz (Regimes I, II) is provided by the pH dependence of the NMRD profiles, Fig. 3. It was found that at high frequency there is no pH dependence, while at low frequency the relaxation rate increases on reducing pH, irrespective of the starting pH. The pH of the ‘as prepared’ BPC and SPC suspensions were ~ 10.1 and ~ 6.0 , respectively. For both types of suspension the accessible pH range was limited by the stability of the colloid. Data are only presented for the pH ranges within which the samples were stable (no precipitation or change in d_{hyd}). We found that SPC suspensions were always more stable to repeated cycling of the pH over the ranges indicated.

Discussion

Formation and morphology of the suspensions

To produce stable BPC suspensions we found that it was critical to take care to remove any non-chemisorbed residues

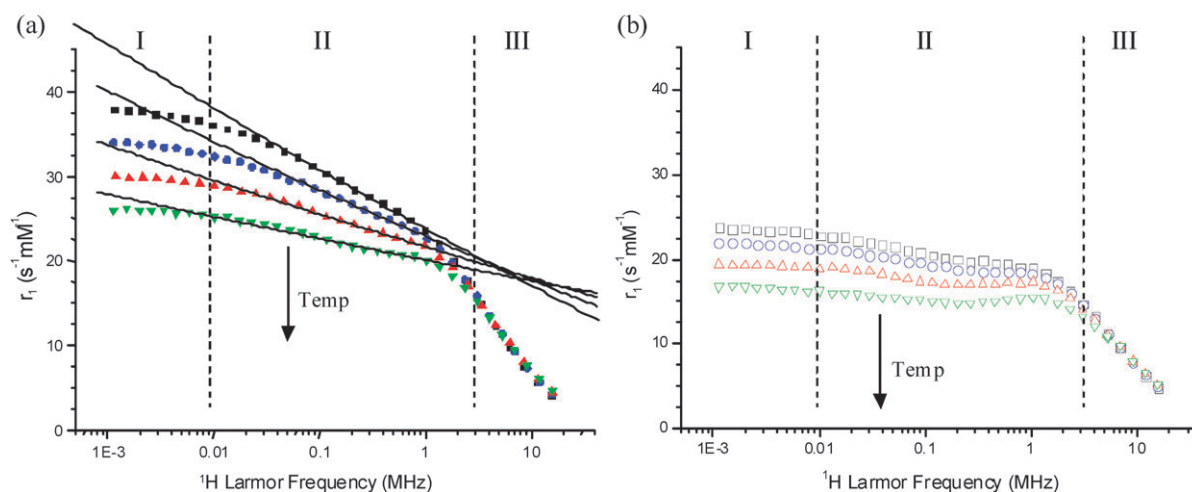


Fig. 2 ^1H NMR relaxation profiles recorded over an extended frequency range as a function of temperature for a typical sodium-oleate stabilised SPC aqueous suspension with d_{hyd} 98 nm, PDI 0.19. (a) In the low temperature range; 20 °C ■, 28 °C ●, 36 °C ▲ and 44 °C ▼. Three relaxation regimes are apparent and the approximate transition frequencies are indicated with dashed lines. The solid lines are fits to the data in Regime II, as discussed in the text. (b) In the high temperature range; 52 °C □, 60 °C ○, 70 °C △ and 80 °C ▽, where the superparamagnetic character of the suspensions becomes apparent.

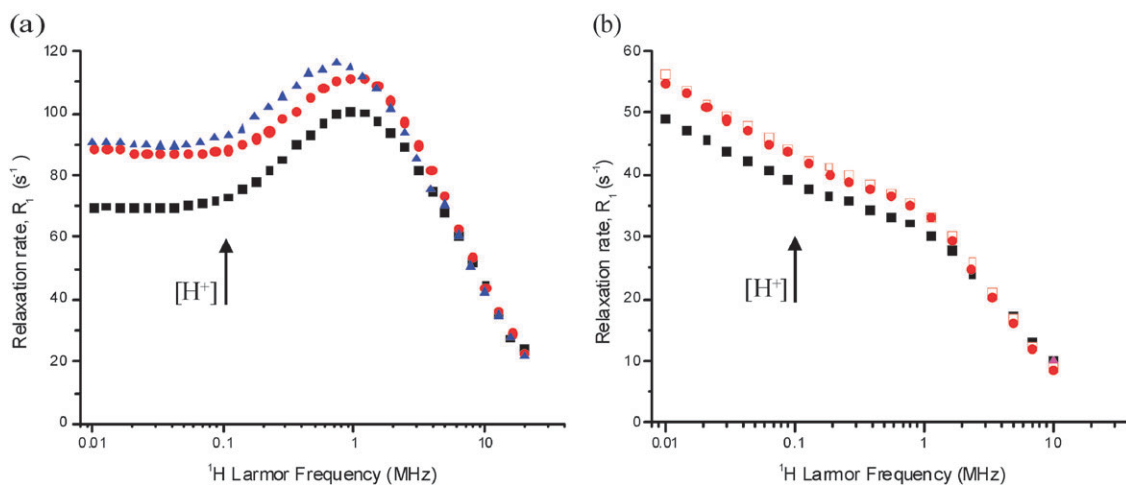


Fig. 3 pH dependence of the relaxation rate, R_1 (not normalised by Fe concentration) of: (a) a decanoic (C10:0) acid, lauric (C12:0) acid stabilised BPC suspension, pH was varied from 10.1 ●, to 9.2 ▲, to 11.0 ■. $[Fe] \sim 6.7$ mM; (b) a decanoic acid stabilised SPC suspension, pH was cycled from 6.0 ■, to 4.9 ●, to 6.0 and back to 4.9 □. $[Fe] \sim 1.7$ mM. pH adjustments were made by addition of small quantities of 1 M HCl and NaOH solutions.

after the co-precipitation step, by precipitation and careful washing with acetone and methanol. We deduce that otherwise a partial second layer of deprotonated fatty acid remains, which is physisorbed onto the primary layer. This partial layer is responsible for the temporary stability of monolayer coated NPs in alkaline solution, but reduces the effectiveness of the subsequent preparation steps. Successive washing of the resulting precipitate reduced the pH close to neutral. A second surfactant could then be applied, as the ammonium or sodium salt of the same, or a different, fatty acid, to form a physisorbed layer. Strong stirring during this coating process at a temperature of 60 °C and subsequent sonication at the same temperature were found to be effective conditions for producing stable suspensions. In suspension the clusters are observed, by PCS, to be stable to dilution with water, or with dilute solutions (25 mM) of the ammonium salt of any fatty acid or sodium oleate, even at a dilution factor of 20, which corresponds to about 0.5 mM iron.

The observed stability of BPC suspensions to dilution with water differs somewhat from the reports of Shen and co-workers.^{10,11} For freshly prepared BPC suspensions the typical iron concentration was *ca.* 12 mM, which corresponds to ~ 0.05 vol% of Fe_3O_4 in the suspension, which we then diluted up to a factor of 20. Shen and co-workers studied comparatively concentrated suspensions (starting in the range of 0.67 vol%) and diluted to a factor of ≥ 4000 . They found the colloids to be stable on dilution to a factor of 100, but on diluting to a factor of 200 ($\sim 5 \times 10^{-3}$ vol%) the colloids were destabilised, resulting in the growth of nanoparticle clusters, which were of lower dimensionality, into the 500 nm range. This was ascribed to the loss of the physisorbed layer on dilution below the CMC of the secondary surfactant (C12:0). In the current work, we have shown that it is possible by controlling the surface coverage, to produce magnetic colloids that are stable to dilution with water down to at least 2.5×10^{-3} vol%, or about four times more dilute than previously found. The improvement observed is moderate, however it does demonstrate the sensitivity of the suspensions to minor

changes in the condition of the fatty acid layers. These observations reflect recent work in our laboratory,²⁷ where controlled reduction in the oleate coverage in the primary layer, by introducing a second solid phase that competes for the stabiliser, was shown to result in controlled cluster growth.

1H NMR relaxation mechanisms in BPC suspensions

The 1H NMR spin–lattice relaxation in BPC suspensions is apparently superparamagnetic in nature, Fig. 1. As noted previously, the simulated profiles conform well with the data when physically reasonable values are used for the saturation magnetisation, M_s , Néel correlation time, τ_N , and anisotropy energy, ΔE_{anis} . The d_{NMR} value, or core size from NMR, of 20 nm, is *ca.* 89% higher than that obtained from TEM. Systematic overestimates of *ca.* 86% were noted by ourselves,¹⁴ for iron oxide NPs of core size ranging from 3 to 7 nm, fully dispersed in heptane. The systematic difference arises in part because SPM theory assumes¹⁵ that the magnetocrystalline anisotropy is uniaxial, and that the Néel process can be characterised using a single correlation time, τ_N .

Alkaline co-precipitation methods are known to produce good crystalline nanoparticles which have saturation magnetisation lower than bulk Fe_3O_4 (80–90 $emu\ g^{-1}$) due to surface effects.²⁸ The value of 27 $emu\ g^{-1}$ obtained from the NMRD analysis of the BPC suspensions is lower than expected. Given the slight sample-to-sample variation evident in Fig. 1a, more detailed simulation suggests that M_s values in the range from 27–31 $emu\ g^{-1}$ can be used to reproduce the experimental curves. Magnetometry measurements on a BPC sample also gave a value of 27 $emu\ g^{-1}$, see ESI.† In previous work we have established¹⁴ that the theory can produce quantitative agreement with M_s values, from magnetometry, for 3–7 nm cores. The work presented here extends the usable size range for NMRD in nanoparticle characterization up to around 11 nm cores. For BPCs the excellent consistency between the physical parameters shows that the suspensions are formed of

clusters of superparamagnetic NPs, with very weak inter-particle interactions.

The agreement between the two techniques arises despite their inherent differences; magnetometry measures the bulk moment, while the ^1H nuclear moments of the water molecules are probes of the surface of the nanostructure. So, for example, in the case of gadolinium-functionalised mesoporous silica,²⁹ the accessibility of the pores within the nanostructure to water was shown to determine the relaxivity. We can conclude therefore that for BPC suspensions all the nanoparticles within the clusters contribute to the water relaxation. Hence the clusters are either in a fluxional state, at room temperature, or their interior is accessible to the solvent molecules. The latter picture is consistent with the fractal dimension of ~ 2.5 (reduced from the maximum of 3 for a 'dense' solid) determined from SANS measurements on BPCs by other groups.¹¹

^1H NMR relaxation mechanisms in SPC suspensions

In Regime III, $\nu_L > 3$ MHz, the relaxation profiles of SPC suspensions are independent of temperature and the data are consistent with the outer-sphere model for relaxation.^{4,16} However, at lower frequency the relaxation at, or slightly above, room temperature confirms that the suspensions are not superparamagnetic in nature, Fig. 2a, indicating the presence of inter-particle interactions. Nor does the relaxation conform a recent extension of SPM theory designed to account for aggregation of superparamagnetic crystals within a permeable coating.³⁰ In that approach the reduced relaxation times are explained as arising from extended water residence times inside the clusters, the relaxation contribution from any given core is assumed to be superparamagnetic. A strong attenuation of the low frequency relaxivity would be expected for clusters in the size range of our SPC suspensions. The fact that this is not observed, Fig. 2, suggests that the water in the environment of the SPCs is not retained for extended times.

In Regime II, $8 \text{ kHz} < \nu_L < 3$ MHz, the relaxivity conforms to a power law dependence on frequency. We have recently reported a similar low frequency response for aqueous magnetite suspensions stabilised with single-stranded DNA,³¹ which we attributed to the presence of very strong inter-particle interactions along the DNA strand. In the case of the DNA stabilised suspensions the low frequency relaxivity was even higher than that reported here, while the power law dependence on frequency was significantly weaker. Similar behavior has also been reported by other groups for core-shell iron-iron oxide nanoparticle clusters,³² which were interpreted in terms of increased magnetic anisotropy associated with the complex composition of the aggregate.

We therefore assign the changes in the profiles, particularly apparent in Regime II at temperatures above 50°C , to the gradual establishment of relaxation due to fluctuations of the nanoparticle magnetic moments on the timescale of T_1 ; which was 4–30 ms in this study. As the temperature is raised thermal energy becomes comparable to the effective anisotropy energy and an increasing fraction of the magnetisation becomes unblocked.³³ We assume that the anisotropic interactions responsible for blocking arise from strong inter-particle

interactions within the clusters, as TEM confirms that the primary particles are in the single-domain size range. These interactions are clearly stronger than in the case of BPCs. From inspection of the profiles in the 1–2 MHz range, Fig. 2b, a r_1 maximum begins to emerge at 70°C . A plot of the temperature dependence of the mid-frequency powers is presented in Fig. 4, this indicates a discontinuity at around 50°C . There is some size dispersity to the cluster size distributions, and presumably some variability in cluster shape. Hence there will be variability in the number, and possibly strength, of inter-particle interactions. We suggest that the value $T_B \approx 50^\circ\text{C}$ is the average temperature at which superparamagnetism becomes evident in SPC suspensions, over the T_1 timescale. Fig. 2 shows that in Regime II, at temperatures below T_B , the value of the power law dependence of the relaxation rate increases with temperature, Fig. 4 shows that the increase is proportional. The observation of a power law dependence of the relaxivity is phenomenological; there is no complete theory for ^1H NMR relaxation arising from the presence of complex magnetic structures of this type. We found that in the accessible temperature range it was not possible to measure a profile for a SPC suspension that conformed to the SPM model. It is also interesting to note that the relaxation profiles obtained for SPCs were insensitive to the samples thermal history, in the temperature range up to 80°C .

The high value for T_B is not without precedence; a blocking temperature of 27°C has been identified from the divergence of the field cooled and zero-field cooled magnetisation curves of hematite nano-assemblies produced by ball-milling,³⁴ while values as high as 0 to 10°C have been determined for $\gamma\text{-Fe}_2\text{O}_3$ by Mossbauer spectroscopy.³⁵ However, to our knowledge this is the first report of the observation of magnetic unblocking of a superparamagnetic nanoparticle assembly by NMR relaxation time analysis.

In Regime I, $\nu_L < 8$ kHz, the relaxivity is independent of frequency. This corresponds to the onset of local sample fields in excess of the external field of the spectrometer. Note that the water relaxation rate remains a function of iron concentration in this regime, so the relevant local fields are the remnant magnetic fields associated with the SPCs. Hence in this

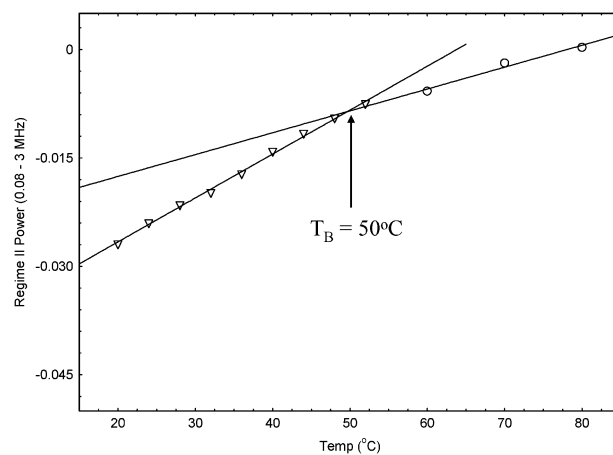


Fig. 4 Temperature dependence of the mid-frequency power for sodium-oleate stabilised SPCs in aqueous suspension. The continuous lines are straight line fits to the data.

frequency range we are measuring the local-field relaxivity, $r_{1\text{loc}}$, as opposed to the spin–lattice relaxivity, r_1 . The transition frequency of 8 ± 2 kHz corresponds to a magnetic field of ~ 0.19 mT. We suggest that the value of the r_1 plateau is a direct measure of the average anisotropy energy of the clusters. The observed temperature dependence of the plateau confirms this interpretation; at higher temperature the low frequency relaxivity decreases as thermal fluctuations become comparable to the height of the barrier. Quantitative interpretation of the data is complicated by the fact that there is no accepted theory for materials of this type. We have, however, shown that it is necessary to measure down into the low kHz range to identify the local-field regime. To our knowledge this is the first reported study of NMR relaxation of magnetic colloids in this frequency range.

Comparison of BPC and SPC suspensions

The physical properties of the two BPC and SPC suspensions studied by NMR are summarised in Table 1. It is apparent that the hydrodynamic sizes and size distributions are similar. TEM analysis shows very similar primary NP sizes, although this is based on measuring relatively small numbers of particles. The fact that the r_1 maximum is at the same frequency for both types of suspension confirms that the population of suspended primary NPs are of approximately the same size.

In the case of BPC suspensions NMRD experiments demonstrate that the ^1H NMR relaxation is superparamagnetic. Hence inter-particle interactions within the clusters are very weak. Dipolar or magnetostatic interactions scale with the square of the moment, so these observations are consistent with the relatively low M_s value determined for these nanoparticles both by magnetometry and NMRD. The reduced crystallinity of nanoparticles from the ‘*in situ*’ preparation as compared to ‘*pre-formed*’ particles of comparable size is most likely due to the introduction of additional surface defects, making the particles more amorphous. However, the effect on the relaxation is dramatic. In the case of SPC suspensions the water relaxation deviates strongly from SPM theory, which is consistent with the presence of stronger dipolar inter-particle interactions within the clusters. NMRD shows that the interactions are stronger for SPCs than those we previously observed for polyelectrolyte (polysodium-4-styrene sulfonate) Fe_3O_4 nanocomposite suspensions.⁹

Table 1 Physical characteristics of the cluster suspensions studied by NMR

Type	BPCs	SPCs
NPs prepared	<i>In situ</i>	Pre-formed
$d_{\text{hyd}}^a/\text{nm}$	82	98
PDI	0.15	0.19
$d_{\text{NP}}^b/\text{nm}$	10.6 ± 1.6	11.4 ± 1.4
$r_{1\text{max}}/\text{MHz}$	1–2	1–2 ^c
^1H NMR relaxation	SPM	non-SPM
$T_B/^\circ\text{C}$	<19	50
$M_s/\text{emu g}^{-1}$	27	58

^a d_{hyd} measured using PCS. ^b d_{NP} average primary nanoparticle size calculated from >100 particle measurements. ^c The maximum was observed at temperatures above 70 °C.

pH dependence and NMR relaxation mechanisms of the suspensions

The changes in r_1 with both pH and temperature confirm the ‘inner sphere’ nature of the relaxation in the sub-MHz range. For BPC suspensions, the outer (physisorbed) surfactant is lauric acid, which has $\text{p}K_a \approx 4.8$.³⁸ Thus, in the relatively narrow pH range (> pH 9) within which we found BPC suspension to be stable (by NMR and PCS), the carboxylate groups of the outer layer are predominantly deprotonated and the clusters are negatively charged. In the case of the SPC suspensions the outer surfactant is oleic acid, which has $\text{p}K_a \approx 4.9$.^{38,39} For a typical freshly prepared SPC suspension, with d_{hyd} 97.1 nm and PDI 0.20, at the ‘as-prepared’ pH of 6.3 the zeta potential was found to be -66.4 mV. On reducing the pH to 4.3, by the addition of 1 M HCl, the size was found to be unchanged, at 98.6 nm, PDI 0.18, and the zeta potential of -14 mV was still negative. So over the pH range studied by NMR the BPC and SPC clusters are negatively charged so the observed pH dependence of R_1 is not due to acid–base behavior of the outer layer surfactants. This is also reasonable when one considers that the carboxylate group may be as much as 3 nm distant from the iron oxide surface.¹⁰ However, as we noted above, it is unlikely that the second layer is 100% complete for both BPC and SPC suspensions, while the high curvature associated with this layer would also be expected to increase the accessibility of the NP surface.

Turning to the inner, chemisorbed layer, both of the fatty acids used occupy relatively high surface area on iron, and other oxides, even when they form a good monolayer. Surface coverage of $20\text{--}25 \text{ \AA}^2$ per molecule has been reported for a range of fatty acids.¹⁰ However, recent work in our laboratory on oleic acid stabilised NPs in heptane suspension²⁷ confirms the presence of a small but identifiable sub-population of vacancies in this layer. We suggest that for BPC and SPCs the amphoteric nature of similar vacant sites results in an increase in the surface proton density at lower pH, providing an additional relaxation pathway through dipolar coupling with the nearby water ^1H nuclei. A similar effect of pH has been observed^{36,37} for ferrihydrite and akaganeite cores in aqueous suspension.

Experimental studies of permeation through lipid bilayers, report water permeabilities for phosphatidyl choline bilayers in the liquid crystal, or expanded, phase in the $10^{-2}\text{--}10^{-3} \text{ cm s}^{-1}$ range.⁴⁰ Comparable data are not available for fatty acid bilayers. However, assuming the same range of permeability and a bilayer depth of 3.0 nm,¹⁰ the approximate timescale for water transport across the bilayer would be $3\text{--}30 \times 10^{-6} \text{ s}$. This is orders of magnitude faster than the pH dependent relaxation rate increases observed for the pH experiments, of $5\text{--}15 \text{ s}^{-1}$, which are equivalent to a reduction in relaxation times of 0.2–0.07 s, Fig. 3. While these are simplistic estimates, they show that amplification of the low frequency ^1H NMR spin–lattice relaxation mechanism due to direct interaction with the NP surface is feasible.

Conclusions/outlook

BPC and SPC suspensions share a great many structural and surface characteristics, however NMRD analysis provides a

clear picture of the factors that influence their magnetic resonance properties. Inter-particle interactions within the clusters are found to determine the low frequency NMR relaxation behaviour. In this frequency range the relaxation mechanism for both types of suspension is inner-sphere in nature, and shows significant pH dependence, a feature which may be possible to exploit in imaging experiments. This study, building on our previous work,^{9,31} establishes low frequency (<8 kHz) relaxivity measurements as a sensitive measure of inter-particle interactions in magnetic nanocomposites, and further develops NMRD as a tool for characterizing dispersed superparamagnetic nanoparticles in suspension. In fact NMRD may be particularly useful in the study of soft assemblies where the magnetic properties are anticipated to be altered on drying. In forthcoming work we will present low frequency NMRD studies of the effect of NP size on the effective magnetic anisotropy in dense magnetic NP clusters in suspension.

Acknowledgements

SG and DC acknowledge Enterprise Ireland (PC/2006/207 and SC/2002/336) for financial support. SC acknowledges Science Foundation Ireland (MASF666). DB acknowledges the Higher Education Authority of the Republic of Ireland and Enterprise Ireland (IF/2001/364, PC/2004/0429) for supporting the purchase of NMR equipment. Finally, we acknowledge Prof. Robert Muller and his colleagues at the University of Mons-Hainault for making their software publicly available.

References

- M. Namdeo, S. Saxena, R. Tankhiwale, M. Bajpai, Y. M. Mohan and S. K. Bajpai, *J. Nanosci. Nanotechnol.*, 2008, **8**, 3247.
- A. M. Derfus, G. von Maltzahn, T. J. Harris, T. Duza, K. S. Vecchio, E. Ruoslahti and S. N. Bhatia, *Adv. Mater.*, 2007, **19**, 3932.
- J.-P. Fortin, F. Gazeau and C. Wilhelm, *Eur. Biophys. J.*, 2008, **37**, 223.
- R. N. Muller, A. Roch, J.-M. Colet and P. Gillis, in *The Chemistry of Contrast Agents in Medical Magnetic Resonance Imaging*, ed. A. E. Merbach and E. Toth, John Wiley and Sons Publishers, 2001, pp. 417.
- S. Laurent, D. Forge, M. Port, A. Roch, C. Robic, L. Vander Elst and R. N. Muller, *Chem. Rev.*, 2008, **108**, 2064.
- C. Khemtong, C. W. Kessinger, J. Ren, E. A. Bey, S.-G. Yang, J. S. Guthi, D. A. Boothman, A. D. Sherry and J. Gao, *Cancer Res.*, 2009, **69**, 1651.
- Y.-W. Jun, Y.-M. Huh, J.-S. Choi, J.-H. Lee, H.-T. Song, S. Kim, S. Yoon, K.-S. Kim, J.-S. Shin, J.-S. Suh and J. Cheon, *J. Am. Chem. Soc.*, 2005, **127**, 5732.
- J.-F. Berret, N. Schonbeck, F. Gazeau, D. El Kharrat, O. Sandre, A. Vacher and M. Airiau, *J. Am. Chem. Soc.*, 2006, **128**, 1755.
- S. A. Corr, Y. K. Gun'ko, R. Tekoriute, C. J. Meledandri and D. F. Brougham, *J. Phys. Chem. C*, 2008, **112**, 13324.
- L. Shen, P. E. Laibinis and T. A. Hatton, *Langmuir*, 1999, **15**, 447.
- L. Shen, A. Stachowiak, K. F. Seif-Eddeen, P. E. Laibinis and T. A. Hatton, *Langmuir*, 2001, **17**, 288.
- M. A. J. Hostenius, T. Niendorf, G. A. Krombach, W. Richtering, T. Eckert, H. Lueken, M. Speldrich, R. W. Gunther, M. Baumann, S. J. H. Soenen, M. De Cuyper and T. Schmitz-Rode, *J. Nanosci. Nanotechnol.*, 2008, **8**, 2399.
- A. Ouakssim, A. Roch, C. Pierart and R. N. Muller, *J. Magn. Mater.*, 2002, **252**, 49.
- C. J. Meledandri, J. K. Stolarczyk, S. Ghosh and D. F. Brougham, *Langmuir*, 2008, **24**, 14159.
- E. Taboada, E. Rodriguez, A. Roig, J. Oro, A. Roch and R. N. Muller, *Langmuir*, 2007, **23**, 4583.
- A. Roch, R. N. Muller and P. Gillis, *J. Chem. Phys.*, 1999, **110**, 5403.
- (a) T. Atanasijevic, M. Shusteff, P. Fam and A. Jasanoff, *Proc. Natl. Acad. Sci. U. S. A.*, 2006, **103**, 14707; (b) L. Josephson, J. M. Perez and R. Weissleder, *Angew. Chem., Int. Ed.*, 2001, **40**, 3204.
- R. McDermott, S. K. Lee, B. ten Haken, A. H. Trabesinger and A. Pines, *Proc. Natl. Acad. Sci. U. S. A.*, 2004, **101**, 7857.
- A. Wooding, M. Kilner and D. B. Lambrick, *J. Colloid Interface Sci.*, 1991, **144**, 236.
- A. Wooding, M. Kilner and D. B. Lambrick, *J. Colloid Interface Sci.*, 1992, **149**, 98.
- (a) X. P. Qiu, *Chin. J. Chem.*, 2000, **18**, 834; (b) R. Massart, *IEEE Trans. Magn.*, 1981, **17**, 1247.
- International Standard ISO13321, Methods for Determination of Particle Size Distribution Part 8: Photon Correlation Spectroscopy, ISO, 1996.
- <http://www.stelar.it/>.
- R. Kimmich and E. Anorado, *Prog. Nucl. Magn. Reson. Spectrosc.*, 2004, **44**, 257.
- E. Anorado and G. M. Ferrante, *Appl. Magn. Reson.*, 2003, **24**, 85.
- M. Koneracka, P. Kopcansky, P. Sosa, J. Bagelova and M. Timko, *J. Magn. Mater.*, 2005, **293**, 271.
- J. K. Stolarczyk, S. Ghosh and D. F. Brougham, *Angew. Chem., Int. Ed.*, 2009, **48**, 175.
- H. M. Lu, W. T. Zheng and Q. Jiang, *J. Phys. D: Appl. Phys.*, 2007, **40**, 320.
- F. Carniato, L. Tei, W. Dastrù, L. Marchese and M. Botta, *Chem. Commun.*, 2009, 1246.
- A. Roch, Y. Gossuin, R. N. Muller and P. Gillis, *J. Magn. Mater.*, 2005, **293**, 532.
- S. J. Byrne, S. A. Corr, Y. K. Gun'ko, J. M. Kelly, D. F. Brougham and S. Ghosh, *Chem. Commun.*, 2004, 2560.
- O. B. Miguel, T. Gossuin, M. P. Morales, P. Gillis, R. N. Muller and S. Veintemillas-Verdaguer, *Magn. Reson. Imaging*, 2007, **25**, 1437.
- T. Jonsson, P. Nordblad and P. Svedlindh, *Phys. Rev. B: Condens. Matter*, 1998, **57**, 497.
- R. A. Borzi, S. J. Stewart, G. Punte, R. C. Mercader, M. Vasquez-Mansilla, R. D. Zysler and E. D. Cabanillas, *J. Magn. Mater.*, 1999, **205**, 234.
- S. Morup and E. Tronc, *Phys. Rev. Lett.*, 1994, **72**, 3278.
- Y. Gossuin, A. Roch, F. Lo Bue, R. N. Muller and P. Gillis, *Magn. Reson. Med.*, 2001, **46**, 476.
- Y. Gossuin, A. Roch, R. N. Muller and P. Gillis, *J. Magn. Reson.*, 2002, **158**, 36.
- The Handbook of Chemistry and Physics*, 67th edn, CRC Press, 1986–1987.
- M. D. Barratt, *Toxicol. in Vitro*, 1996, **10**, 85.
- S.-J. Marrink and H. J. C. Berendsen, *J. Phys. Chem.*, 1994, **98**, 4155.